Localized Turbulence Suppression and Increased Flow Shear near the $q = 2$ Surface during Internal-Transport-Barrier Formation

M. W. Shafer,[1] G. R. McKee,[1] M. E. Austin,[2] K. H. Burrell,[3] R. J. Fonck,[1] and D. J. Schlossberg[1]
[1]University of Wisconsin-Madison, 1500 Engineering Drive, Madison, Wisconsin, 53706, USA
[2]University of Texas-Austin, 1 University Station, Austin, Texas 78712, USA
[3]General Atomics, P.O. Box 85608, San Diego, California 92186-5608, USA
(Received 28 January 2009; published 14 August 2009)

Broadband turbulent fluctuations in the plasma density are transiently suppressed when low-order rational q surfaces first appear in negative central magnetic shear plasmas on the DIII-D tokamak, which can lead to the formation of internal transport barriers. Increased localized flow shear is simultaneously observed. It transiently exceeds the measured turbulence decorrelation rate, providing a mechanism to trigger the formation of the transport barrier. This increased flow shear and turbulence suppression propagates radially outward, following the $q = 2$ surface.

DOI: 10.1103/PhysRevLett.103.075004 PACS numbers: 52.35.Ra, 52.25.Fi, 52.30.−q, 52.55.Fa

The complex dynamics between pressure-gradient driven turbulence, local transport, and equilibrium and self-generated sheared flows are crucial to the confinement and overall performance of magnetically confined toroidal plasmas. Under some conditions, this interplay may suppress turbulence in the plasma interior, giving rise to an internal transport barrier (ITB), which is of great interest because it increases the plasma pressure and thus fusion performance [1]. The geometry of the confining helical magnetic fields is found to be of central importance to ITB formation and is quantified by the safety factor, q, defined as the ratio of the change in toroidal magnetic flux with poloidal flux. In discharges with an off-axis minimum in q, an ITB can be triggered at the appearance of low-order rational values of the minimum q, $q_{\min}$ [2–7].

Several experimental results suggest increased $\boldsymbol{E} \times \boldsymbol{B}$ shear flow develops in the region of $q_{\min}$ before core barrier formation, thereby reducing drift-wave-like transport and forming an ITB [2,8]. More recently, numerical simulations with the nonlinear gyrokinetic code, GYRO [9], predict increased zonal flows near integer q minima in reversed shear plasmas [10]. Secondary convective cells (low m, n modes where m, n are the poloidal and toroidal mode numbers, respectively) have also been theorized to develop a sheared flow structure near integer q values at low magnetic shear [magnetic shear is the normalized radial gradient of q and is defined as $\hat{s} = (r/q)dq/dr$], providing the $\boldsymbol{E} \times \boldsymbol{B}$ velocity shear necessary to suppress turbulent transport and thus trigger an ITB [11,12]. However, the relation of low-order rational values of $q_{\min}$ to turbulence and transport in the context of ITB formation has not yet been experimentally demonstrated.

In this Letter, for the first time in the core regions of a high-temperature tokamak plasma, we present simultaneous measurements of local plasma turbulence intensity, decorrelation rates, and radially sheared poloidal flows at high temporal and spatial resolution (5 ms and 1 cm, respectively) that demonstrate the connection between increased flow shear, transient local turbulence suppression, increased temperatures, and the global magnetic equilibrium of the plasma. These sheared flows are found following the appearance of a low-order rational (usually integer) $q_{\min}$ surface and they appear to be damped by magnetic shear. At the time a $q_{\min} = 2$ surface first appears, a reduction in the intensity of localized low-wave number fluctuations near the $q_{\min} = 2$ surface is observed and is coincident with the development of a sheared poloidal velocity layer linked to the $q = 2$ surface (in the absence of MHD activity). While measurements of the reduction in turbulent fluctuations during an ITB have been reported [13–15], the localization to the $q_{\min} = 2$ surface and coexistence with enhanced localized shear flow is of central importance to the process and has not been previously observed.

The measurements were obtained in negative central magnetic shear (NCS) [16] low-density L-mode discharges on DIII-D with: $P_{inj} = 5$ MW (neutral beam injection), $I_p = 1.2$ MA, $B_T = 2$ T, $n_e \sim 2 \times 19$ m^{-3}, $\beta_n \sim 0.6$. Two discharge conditions are examined and compared: high toroidal rotation, ν_ϕ, with all co-current neutral beam injection and low ν_ϕ with balanced neutral beam injection. Given the central importance of the safety factor profile and evolution, $q(r, t)$, direct and indirect measurements of q are corroborated from multiple diagnostics: motional stark effect (MSE), CO_2 interferometry, far-infrared scattering (FIR), and electron cyclotron emission (ECE). A more complete description of this discharge scenario is found in Ref. [7].

As the discharge evolves, discrete localized transient increases in the ion temperature, T_i, and electron temperature, T_e, are observed when low-order rational values of $q_{\min}$ ($q_{\min} = 4, 3, 2$) enter the plasma. Here, a transient off-axis $q_{\min}$ moves radially inward and decreases with time. At the time that $q_{\min} = 2$, a sustained ITB can be triggered

in the T_i, T_e, and ν_ϕ profiles and is most pronounced in the core ($r/a < 0.3$) for these discharges. Once the ITB is triggered by the appearance of the integer $q_{\min}$ surface, the barrier can be sustained provided that sufficient equilibrium $\boldsymbol{E} \times \boldsymbol{B}$ shear is available. The equilibrium $\boldsymbol{E} \times \boldsymbol{B}$ shear in plasmas with balanced neutral beam injection (low ν_ϕ) was found to be insufficient for barrier formation, though transient turbulence suppression and temperature increases are also observed [17]. These features can be seen in Fig. 1, which shows the T_i and ν_ϕ at two different radii (core and midradius) for both ν_ϕ cases.

The time at which the $q_{\min} = 2$ surface first appears in the plasma can been determined to ± 2 ms by measurements of reverse shear Alfvén eigenmode (RSAE) cascades [18,19]. Multiple modes are excited simultaneously when low-order rational $q_{\min}$ values enter the plasma and can be measured by several density fluctuation diagnostics (FIR, CO_2 interferometry, beam emission spectroscopy).

This is found to be coincident with the appearance of a sharp transient increase in ∇T_e measured by ECE [7]. Thus, the ∇T_e increases give an estimate of the $q_{\min} = 2$ time (usually ± 3 ms), but also give an estimation of the radial location of the $q = 2$ surfaces as they propagate radially inward and outward from the minimum (see Fig. 9 of Ref. [7]). This effect, which has also been seen on JET [20] and JT-60U [21], has been corroborated against MSE measurements on DIII-D [7]. This is valuable given the uncertainty in the position of $q_{\min}$ for weakly reversed shear profiles like the discharges presented here. These locations can generally be determined within ± 2.3 cm, corresponding to $\Delta r/a = \pm 0.04$ (± 1 ECE channel).

Figure 2(a) illustrates the spatially and temporally resolved electron temperature gradient for a high ν_ϕ discharge (shot 126 582). Here, transient increases in ∇T_e originate near the $q_{\min}$ surface ($r/a = 0.42 \pm 0.04$) and quickly propagate in a wavelike fashion radially inward and outward with the $q = 2$ surface and extend across the region, $0.0 < r/a < 0.7$, where r is the radius and a is the minor radius. This propagation is shown more clearly in the inset in Fig. 2(a) where the arrow is used as a guide. Dashed lines indicate the time $q_{\min} = 3$, 2. Here, the $q_{\min} = 2$ time via RSAEs was determined to be 1135 ± 5 ms and 1137 ± 3 ms via ∇T_e.

The turbulence and poloidal flow measurements presented here were obtained with the beam emission spectroscopy (BES) diagnostic [22]. The BES diagnostic measures localized, long wavelength ($k < 3$ cm^{-1}) two-dimensional density fluctuations with 30 channels deployed in a 5×6 grid in the radial/poloidal plane along the outboard midplane. Each channel is separated by approximately 1 cm, which translates to $\Delta r/a = 0.016$ in the plasma. Poloidal flow velocity measurements of the turbulence are calculated via time-delay cross-correlations between poloidally separated channels. This measures the lab-frame turbulent eddy advection velocity [23]. Typically in DIII-D, the $\boldsymbol{E} \times \boldsymbol{B}$ velocity dominates the turbulence advection such that effects of the diamagnetic velocity (<1 km/s) in the laboratory frame are minimal.

Figure 2(b) illustrates a low-k turbulence spectrogram at $r/a = 0.48$. The upward shift in frequency with time is due primarily to increasing Doppler shift as ν_ϕ and the associated radial electric field increase as the discharge evolves. A sharp reduction in the turbulence amplitude is clearly observed around the time $q_{\min}$ crosses 2. A similar,

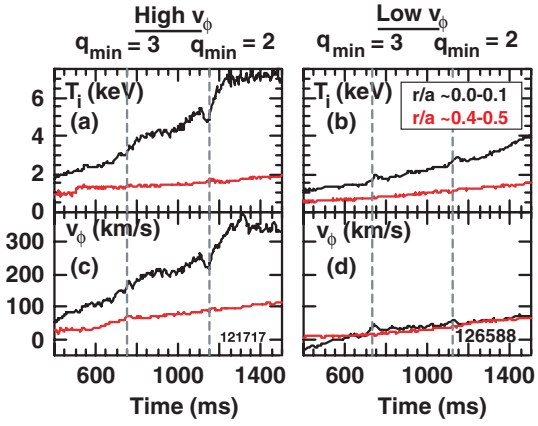

FIG. 1 (color online). T_i in the core ($r/a \sim 0.0$–0.1) and at midradius ($r/a \sim 0.4$–0.5) at high ν_ϕ (a) and low ν_ϕ (b). Toroidal rotation for high ν_ϕ (c) and low ν_ϕ (d). Vertical dashed lines denotes the time that $q_{\min} = 2$, 3.

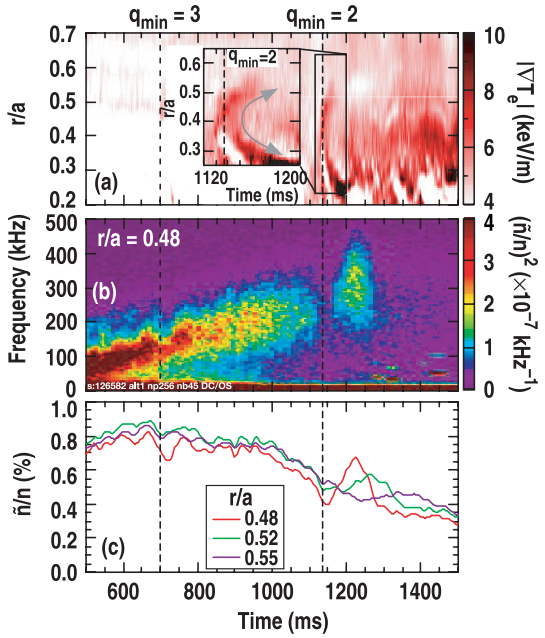

FIG. 2 (color online). (a) ∇T_e measured by ECE. (b) Density fluctuation power spectrum at $r/a = 0.48$. (c) Radially separated density fluctuation levels, $\tilde{n}/n$. The radial location of the $q_{\min} = 2$ surface is $r/a = 0.42 \pm 0.04$.

but less pronounced, reduction is also observed when $q_{\min}$ crosses 3.

The integrated density fluctuation levels for three nearby radial locations ($0.48 \leq r/a \leq 0.55$) are shown in Fig. 2(c) with a time resolution of 5.8 ms. The fluctuation levels vary over time due to evolving equilibrium conditions. Starting at 1100 ms, the fluctuation levels decrease by 30% at $r/a = 0.48$. This point is noted by a break in the slope of the evolving fluctuation levels. Thus, the fluctuations start to decrease roughly 35 ms before the $q_{\min} = 2$ time, indicating that effects leading to a barrier formation occur prior to appearance of the $q_{\min} = 2$ surface. Simulations with the GYRO code suggest increased zonal flow activity with $q_{\min}$ near 2 [7,10], consistent with these observations. The fluctuation levels radially outward from the location of $q_{\min}$ exhibit a more modest reduction following the time the $q_{\min} = 2$ surface appears. The reductions in the fluctuation levels at the outer radii also occur later in time, indicating outward radial propagation of the suppression layer. Based on the ∇T_e increases from Fig. 2(a), the $q = 2$ surface is found to propagate faster than these reductions. Similar reductions in the density fluctuations are observed in low rotation plasmas, where the propagation speeds are slightly faster and closer to the $q = 2$ surface.

While the minimum in fluctuations nearest the $q_{\min}$ radius occurs coincident with the ∇T_e increases, the relation between reduced fluctuations and increased temperature is more complex at the outer radial locations, indicating a complicated dynamic between turbulence and transport. High-frequency zonal flows, for example, may play a role yet be outside of the measurement sensitivity limits.

Following this sharp decrease in the fluctuation levels for $q_{\min} = 2$ is a subsequent increase in fluctuation level, the largest of which occurs at $r/a = 0.48$ around 1230 ms. This transient growth in turbulence fluctuation levels may reflect a nonlinear coupling of multiple coaligned turbulence modes at the rational surface [24] as the $q = 2$ surface passes through the BES sampling area. However, based on an estimate of the radial propagation of the ∇T_e increases, the $q = 2$ surface travels at a slightly faster radial velocity than the rise in turbulence.

Poloidal flow perturbations are observed in the turbulence flow velocity near the $q_{\min} = 2$ surface. The perturbations are shown in Fig. 3 for the high (a) and low (b) ν_ϕ cases. The radial locations of the $q_{\min} = 2$ surface for these discharges are $r/a = 0.46 \pm 0.04$ for the high ν_ϕ case and $r/a = 0.33 \pm 0.04$ for the low ν_ϕ case (based on ∇T_e). This data was assembled over 3 discharges for each case. In both cases a large perturbation in the poloidal turbulence flow is detected at or just outside the $q = 2$ surface following the time that $q_{\min} = 2$. This perturbation propagates radially outward at a speed near 1 m/s in the high ν_ϕ case and ~1.3 m/s in the low ν_ϕ case. Both of these propagation speeds lag behind the outward propagation speed of the ∇T_e increases of 2–3 m/s.

The radially localized poloidal velocity perturbations create a transient zone of high poloidal velocity shear.

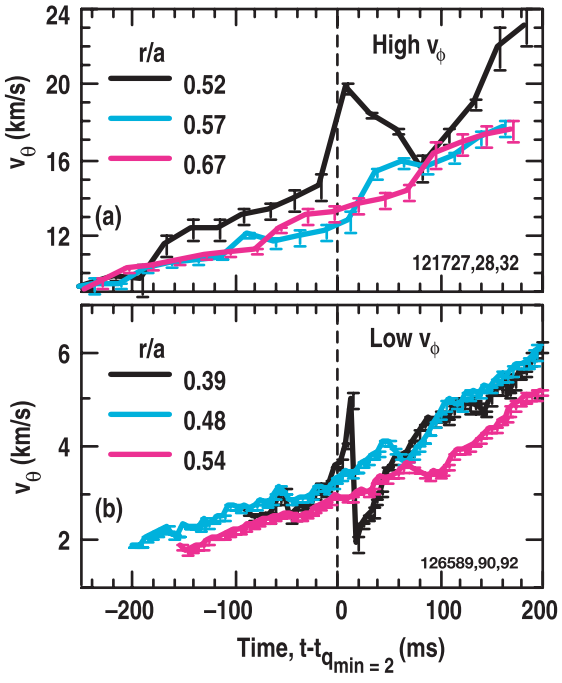

FIG. 3 (color online). Poloidal flow measured by turbulence advection at high ν_ϕ (a) and low ν_ϕ (b). The radial location of the $q_{\min} = 2$ surface is $r/a = 0.46 \pm 0.04$ for the high ν_ϕ case and $r/a = 0.33 \pm 0.04$ for the low ν_ϕ case.

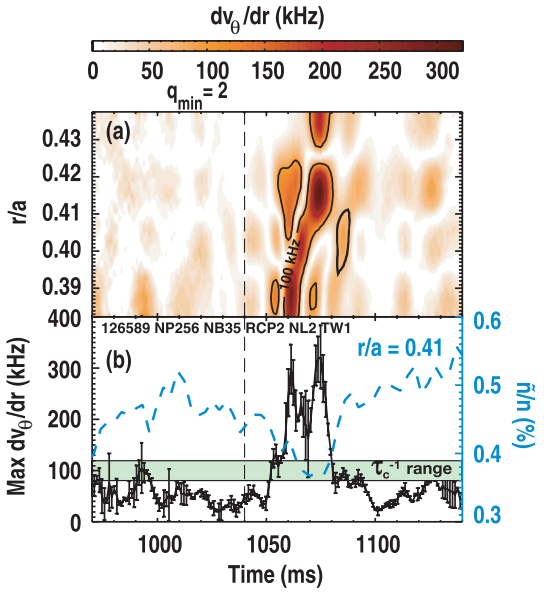

FIG. 4 (color online). (a) Radially sheared poloidal flow rate of turbulence at low ν_ϕ. (b) Maximum shear rate from part (a) compared to measured turbulence decorrelation rate. Local density fluctuation level is on the right axis in a dashed blue line.

For the high ν_ϕ case, the estimated poloidal velocity shear rate ($\omega_s = d\nu_\theta/dr$) exceeds 500 kHz. The transient shear rate for the low ν_ϕ case was measured to peak at over 300 kHz. The decorrelation rate of the turbulence is calculated as the exponential decay rate from cross-correlations of poloidally displaced BES channels [23]. Here, τ_c^{-1} is $\sim$85 kHz $\pm$ 15 kHz for high ν_ϕ and $\sim$100 $\pm$ 20 kHz at low ν_ϕ. Hence, the localized shearing rate transiently satisfies the condition for suppressing turbulence, $\omega_s > \tau_c^{-1}$ [25,26] and is thus sufficient to reduce turbulence, as is observed. This alone cannot justify a sustained barrier, but is consistent with a possible trigger mechanism.

The measured evolution and structure of the velocity shear is shown in Fig. 4 for the low ν_ϕ case. The radial velocity shear in Fig. 4(a) is found to propagate outward from the $q_{\min} = 2$ surface at $r/a = 0.33 \pm 0.04$, creating a maximum shear that is sustained at a value greater than the measured decorrelation rate for 30 ms, as indicated in Fig. 4(b). Localized density fluctuations at $r/a = 0.41$ are also plotted in Fig. 4(b) in blue on the right axis. Here, the minimum in the fluctuations corresponds with the maximum in the shear rate and is located in the region of maximum velocity shear. The high ν_ϕ case shows a similar result, demonstrating the universality of the turbulence interaction with low-order q surfaces, despite the significantly different barrier evolution after the event.

Both the axisymmetric zonal flow and the low m, n convective cell show qualitative similarities to the turbulence measurements presented here. Both flows are predicted to provide an oscillatory flow shear stabilization. GYRO simulations suggest zonal flows arise due to a resonance of turbulent modes that occur on either side of $q_{\min}$, when $q_{\min} = 2$ [10]. The radial gradient of these modes nonlinearly drives zonal flows inside and outside the $q_{\min} = 2$ surface. Theorized convective cells are predicted to form in regions surrounding minimum q (zero magnetic shear) and then to decay quickly with increasing magnetic shear [12]. We also note the striking similarity between the transient shear flow presented here and large E_r shear observed near $q_{\min}$ in ERS plasmas on TFTR; a similar mechanism may well be at play in both scenarios [8]. Other physical mechanisms may also play a role in shear flow generation near low-order rational-q surfaces in some discharge scenarios. Double tearing modes [27], for example, have been associated with ITB formation. However the discharges presented here did not show MHD activity so this process is not active in these particular plasmas.

In summary, simultaneous measurements of turbulence intensity and poloidal velocity demonstrate a clear reduction in long wavelength density turbulence that coincides with enhanced shear flows that transiently exceed the turbulence decorrelation rate. This phenomena may partially or wholly explain the formation of an NCS ITB at the appearance of $q_{\min} = 2$. These effects are strongest near the $q_{\min} = 2$ surface and are found to track behind the $q = 2$ surface as it propagates radially outward, consistent with simulations suggesting increased zonal flow or convective cell activity in this region.

The authors thank the DIII-D program for its support of this scientific collaboration and Chris McDevitt and Ron Waltz for useful discussions. This work is supported by US DOE under DE-FG02-89ER53296, DE-FG03-97ER54415, and DE-FC02-04ER54698.

[1] R. C. Wolf, Plasma Phys. Controlled Fusion **45**, R1 (2003).
[2] Y. Koide and M. Kikuchi, Phys. Rev. Lett. **72**, 3662 (1994).
[3] C. L. Rettig *et al.*, Phys. Plasmas **5**, 1727 (1998).
[4] M. G. Bell *et al.*, Plasma Phys. Controlled Fusion **41**, A719 (1999).
[5] E. Joffrin, C. D. Challis, T. C. Hender, D. F. Howell, and G. T. A. Huysmans, Nucl. Fusion **42**, 235 (2002).
[6] S. Günter *et al.*, Nucl. Fusion **41**, 1283 (2001).
[7] M. E. Austin *et al.*, Phys. Plasmas **13**, 082502 (2006).
[8] R. E. Bell, F. M. Levinton, S. H. Batha, E. J. Synakowski, and M. C. Zarnstorff, Phys. Rev. Lett. **81**, 1429 (1998).
[9] J. Candy and R. E. Waltz, J. Comput. Phys. **186**, 545 (2003).
[10] R. E. Waltz, M. E. Austin, K. H. Burrell, and J. Candy, Phys. Plasmas **13**, 052301 (2006).
[11] P. H. Diamond, Ö. D. Gürcan, C. J. McDevitt, and M. A. Malkov in *Proceedings of the 21st IAEA Fusion Energy Conference, TH/2-4 (2006)*, http://www-pub.iaea.org/MTCD/Meetings/FEC2006/th_2-4.pdf
[12] C. J. McDevitt and P. H. Diamond, Phys. Plasmas **14**, 112306 (2007).
[13] E. Mazzucato *et al.*, Phys. Rev. Lett. **77**, 3145 (1996).
[14] C. M. Greenfield *et al.*, Nucl. Fusion **39**, 1723 (1999).
[15] G. D. Conway *et al.*, Plasma Phys. Controlled Fusion **43**, 1239 (2001).
[16] E. J. Strait *et al.*, Phys. Rev. Lett. **75**, 4421 (1995).
[17] M. E. Austin *et al.*, in *Proceedings of the 21st IAEA Fusion Energy Conference, EX/P3-1 (2006)*, http://www-pub.iaea.org/MTCD/Meetings/FEC2006/ex_p3-1.pdf
[18] S. E. Sharapov *et al.*, Phys. Rev. Lett. **93**, 165001 (2004).
[19] M. A. Van Zeeland *et al.*, Phys. Rev. Lett. **97**, 135001 (2006).
[20] E. Joffrin *et al.*, Plasma Phys. Controlled Fusion **44**, 1739 (2002).
[21] S. V. Neudatchin *et al.*, Nucl. Fusion **44**, 945 (2004).
[22] D. K. Gupta, R. J. Fonck, G. R. McKee, D. J. Schlossberg, and M. W. Shafer *et al.*, Rev. Sci. Instrum. **75**, 3493 (2004).
[23] R. D. Durst, R. J. Fonck, G. Cosby, and H. Evensen, Rev. Sci. Instrum. **63**, 4907 (1992).
[24] B. A. Carreras, K. Sidikman, P. H. Diamond, P. W. Terry, and L. Garcia, Phys. Fluids B **4**, 3115 (1992).
[25] K. H. Burrell, Phys. Plasmas **4**, 1499 (1997).
[26] P. W. Terry, Rev. Mod. Phys. **72**, 109 (2000).
[27] J. Q. Dong, Z. Z. Mou, Y. X. Long, and S. M. Mahajan, Phys. Plasmas **11**, 5673 (2004).